Volume 16, Issue 3, 162524 (1-12)

International Journal of Nano Dimension (IJND)

https://dx.doi.org/10.57647/j.ijnd.2025.1603.24

Effect of reinforcements, temperature and defect on mechanical properties of aluminum nanocomposites reinforced with carbon nanotube and graphene: A molecular dynamics study

Wijdan Qahtan Farhan Al-Humairi, Samrand Rash-Ahmadi*, Mortaza Khalilian

Department of Mechanical Engineering, Urmia University, Urmia, Iran.

***Corresponding author:** s.rashahmadi@urmia.ac.ir

Original Research

Received:
13 November 2024
Revised:
8 December 2024
Accepted:
29 January 2025
Published online:
1 June 2025

Abstract:

Numerous industries widely utilize aluminum metal because of its excellent properties. Therefore, enhancing the strength and tensile strength of aluminum holds significant importance. In this study, molecular dynamics simulation was used to investigate the effect of increasing the number of graphene nanosheets and carbon nanotubes with defects and without defects in the aluminum matrix under different temperatures. The simulation results show that by adding the number of reinforcements (1 to 4) to the aluminum matrix, the Young's modulus of the nanocomposites improved for graphene nanosheets (88 to 252 GPa) and carbon nanotubes (79 to 138 GPa). Also, the presence of defects in graphene nanosheets and carbon nanotubes reduces Young's modulus and tensile strength of aluminum nanocomposites. In addition, as the temperature of nanocomposites increased (250 to 500° K), the tensile strength and Young's modulus decreased. The results of this study provide a more comprehensive understanding of the mechanical properties and behavior of aluminum nanocomposites reinforced with several graphene nanoplates and carbon nanotubes.

Keywords: Aluminum nanocomposites; Carbon nanotubes; Defects; Graphene; Mechanical properties; Nanocomposites

1. Introduction

Aluminum is one of the many metals in the world [1]. Due to its low weight [2], high flexibility [3], and high heat transfer [4], construction of household appliances [5], packaging and food storage [6]. But one of the biggest disadvantages of aluminum is its strength and tensile strength [7], which is much lower than other metals. Recently, nanocomposites have been used more extensively in various fields, including biomaterial [8–10] and coating [11]. Significant efforts have been made to enhance the properties of metal-based composite nanostructures [12]. On the other hand, carbon allotropes (graphene and carbon nanotubes) have been used as reinforcements in many composites, including polymer composites [13–17], metal composites [18–22] and ceramic composites [23]. Due to their high strength [24–26] and low weight [27], high tensile strength [28], they have played an important role in the mechanical properties of composites. According to previous studies by Jiang et al. [29] on the mechanical properties of aluminum nanocomposites reinforced with graphene. By adding graphene reinforcement to the aluminum matrix, the tensile strength improved from 233 to 287 MPa. In addition, the study of Morovvati et al. [30] showed the mechanical properties of aluminum composites. By adding two percent of the weight of carbon nanotubes to the aluminum matrix, elastic module improved from 67488.53 MPa to 73720.59 Mpa. The study of molecular dynamics by Li et al. [31], shows that the fracture stress of the composite increased from 55.5 to 595 GPa compared to pure aluminum. The study of Azizi et al. [32], shows that the addition of 0.5 weight percentage of graphene to the aluminum matrix increased the fatigue life of the composite by 234% at the low stress level and by 44% at the high stress level. Also, strengthening the aluminum matrix with carbon nanotubes can improve the plasticity of nanocom-

posites [33]. Choi et al. [34] showed in a molecular dynamics study that the addition of $4*4$, $6*6$, and $8*8$ carbon nanotubes to the aluminum matrix increases the Young's modulus by 31%, 33%, and 39%, respectively. Khanna et al. [35] an experimental study showed that by adding 25.0% graphene to the aluminum matrix, the hardness and maximum compressive stress of the composite are 98.2% and 59.1% higher than the aluminum matrix, respectively. With increasing temperature in aluminum nanocomposites reinforced with carbon nanotubes, the Young's modulus decreases by 11.7% [36]. The results of Dixid et al. [37] in an experimental study showed that adding several layers of graphene to the aluminum matrix leads to a two-fold improvement in strength without losing the plasticity of the composite. The distribution effect of graphene in the aluminum matrix is very important; as the angle between graphene and the stretching direction increases, the tensile stress of the system tends to decrease [38]. Wang et al. [39] in a molecular dynamics study showed that the presence of graphene layers in the aluminum matrix has a great effect on the ultimate strength, Young's modulus, and the fracture strain of the composite.

Theoretical predictions of the mechanical properties always have significant errors due to limitations in model and environmental conditions compared to experimental results. However, molecular dynamics simulations provide more accurate predictions of the mechanical properties of nanocomposites due to the compatibility of different conditions. In this work, molecular dynamics simulation was used to investigate the effect of increasing the number of graphene layers as well as carbon nanotubes with and without defects on the mechanical properties of aluminum composites under different temperatures. According to the works done in the previous literature, it was necessary to investigate these cases.

2. Materials and methods

2.1 Modeling of aluminum nanocomposites reinforced with graphene and carbon nanotubes

In this first part, the aluminum matrix was modeled in dimensions of $30 \times 30 \times 25$ angstroms. Then, according to the type of composite, graphene nanosheets and carbon nanotubes were added. Also, to prevent overlapping of carbon atoms with aluminum atoms, aluminum atoms that had a distance of less than 1.2 angstroms with carbon atoms were removed. Also, graphene nanoplates (GNs) and carbon nanotubes (CNT) were placed next to each other in an aluminum matrix at a distance of 2.5 angstroms. The nanocomposites were modelled with dimensions of $30 \times 30 \times 25$ Å. Graphene nanosheets with dimensions 30×30 Å were added to the aluminum matrix in single, double, triple, and quadruple layers. Also, carbon nanotubes 4×4 reinforcements with a length of 30 Å were added to the aluminum matrix in the form of 1 to 4 nanotubes. For carbon nanotubes (4,4), dimensions of a length of 30 angstroms were used. It was also used as an armchair for graphene nanoplates with dimensions of 30×30 angstroms. Also, the percentage of defects was randomly added efficiently (1% per nanoplates) to graphene nanoplates and carbon nanotubes. Figure 1 shows the shape of a graphical representation of the modeled composites. Also, figure 2 shows graphical output of the nanocomposite models.

2.2 Force fields

For the force potentials between aluminum matrix atoms and graphene nanoplates and carbon nanotubes, Tersoff [40] and EAM [41] potential functions were used. For the interactions between carbon atoms in graphene nanosheets and carbon nanotubes, the Tersoff potential function was used. EAM potential function was also used for interactions between aluminum atoms. Also, for the potential function interactions for nanocomposite, the sum of these two potential functions was used as a hybrid overlay. Equation 1 shows the equation of the Tersoff potential function, and equation 2 shows the equation of the EAM potential function.

$$E = \frac{1}{2}\sum_{i}\sum_{i\neq j} V_{ij} \tag{1}$$

E (Kcal/mol) denotes the energy of system. V_{ij} (Kcal/mol) signifies the binding energy.

$$E_i = F_a\left(\sum_{i\neq j}\rho_\beta(r_{ij})\right) + \frac{1}{2}\sum_{i\neq j}\phi_{\alpha\beta}(r_{ij}) \tag{2}$$

where $\phi_{\alpha\beta}$ is a pair-wise potential function, r_{ij} is the distance between atoms i and j, ρ_β represents how much the

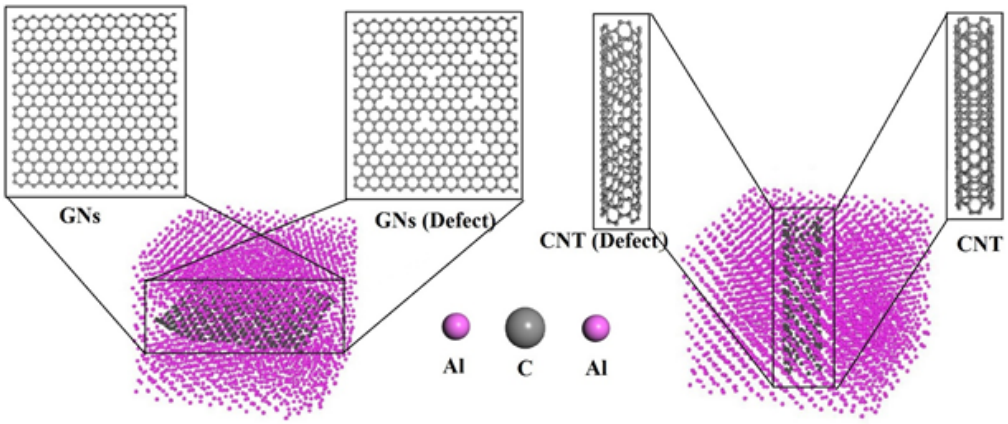

Figure 1. Graphical output of the nanocomposite and reinforcement models.

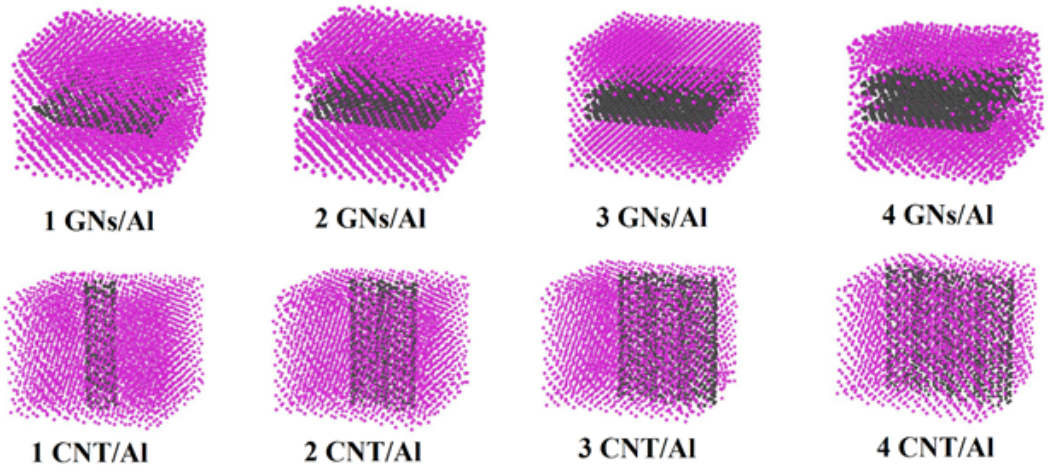

Figure 2. Graphical output of the nanocomposite models.

atom contributes to the electron charge density and F is a function that provides the energy needed to position atom i of type α in the electron cloud.

2.3 Details of simulation

For the simulation and aluminum nanocomposite reinforced with carbon nanotubes and graphene nanosheets, the open-source code of Lammps [42] was used. Boundary conditions were considered periodic for the whole nanocomposite in all three directions. To relax the tension in the system, the NVT ensemble (constant volume and temperature) was used. In addition, the energy of the system was minimized before the run of the tensile load. Also, the time step for all simulations was considered 0.001 ps. To investigate the mechanical properties of nanocomposites, all nanocomposites were subjected to axial tension (0.1 ps). The molecular dynamics simulation algorithm converges based on the number of simulation repetitions (runs). In this study, we conducted a total of 100×10^3 runs. Additionally, the simulations were repeated multiple times to ensure a certain level of convergence.

2.4 The critical energy release rate of composite models

Equation 4 is used to calculate the critical energy release rate (Gc), with equation 3 defining ΔU as the potential energy of a fully cracked system. In this context, U_i represents the potential energy before crack initiation, and U_f refers to the potential energy after the crack has formed. Additionally, according to equation 4, t denotes the thickness of the nanocomposites, which in this study is taken as 25 Å. Furthermore, Δa in this study represents the change in crack length.

$$\Delta U = U_f - U_i \tag{3}$$

$$G_c = \frac{\Delta U}{t\Delta a} \tag{4}$$

3. Results and discussions

3.1 The effect of the number of reinforcements on the mechanical properties of aluminum nanocomposite

Figure 3 shows the stress-strain curves of aluminum nanocomposites reinforced with several graphene nanoplates. According to figure 3 (a), with increasing the number of layers from 1 to 4 to the aluminum matrix,

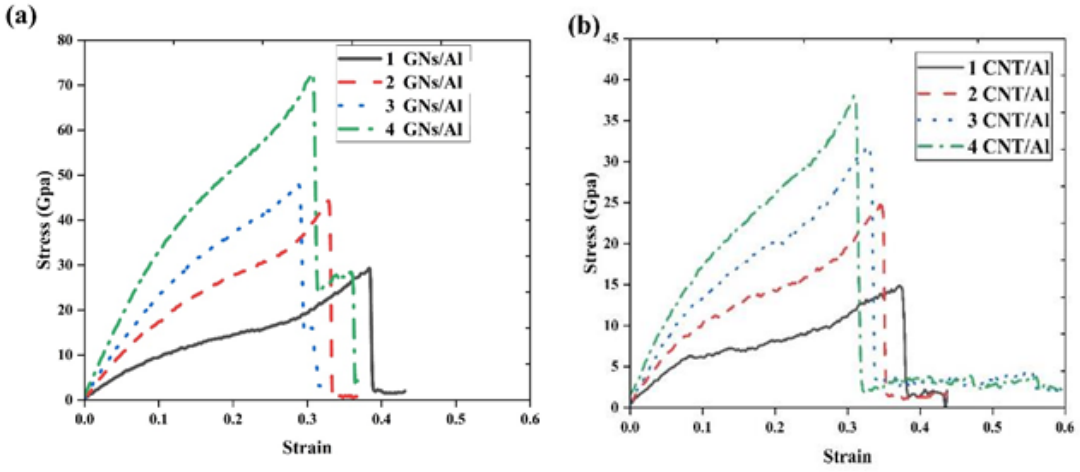

Figure 3. The stress-strain curves of aluminum nanocomposites reinforced with several graphene nanoplates and carbon nanotubes (a) GNs/Al nanocomposites (b) CNT/Al nanocomposites.

the strength of the nanocomposite increases. Also, in figure 3 (b), by adding the number of carbon nanotubes, the strength of the nanocomposite increases. In addition, figures 4 and 5 also show the Young's modulus and tensile strength of the nanocomposite under the number of graphene and carbon nanotube reinforcements, respectively. According to figure 4 (a), the highest Young's modulus of the aluminum nanocomposite reinforced with 4 layers was 252 GPa. Also, the lowest Young's modulus of the aluminum nanocomposite reinforced with one layer of graphene nanoplate was 88 GPa. The results of these graphs show that the amount of Young's modulus increases with the increase in the number of graphene layers in the aluminum nanocomposite. Also, figure 4 (b), shows Young's modulus of nanocomposites reinforced with carbon nanotubes. According to this diagram, with the addition of carbon nanotubes to the aluminum matrix, the Young's modulus increases from 79 to 138 GPa.

In addition, figure 5 shows the tensile strength of aluminum nanocomposites reinforced with graphene nanoplates and carbon nanotubes. According to the graphs in figure 5 (a), with the increase in the number of graphene layers, the tensile strength improved from 28 to 74 GPa. Also, according to figure 5 (b), by increasing the number of carbon tubes in the aluminum matrix, the tensile strength

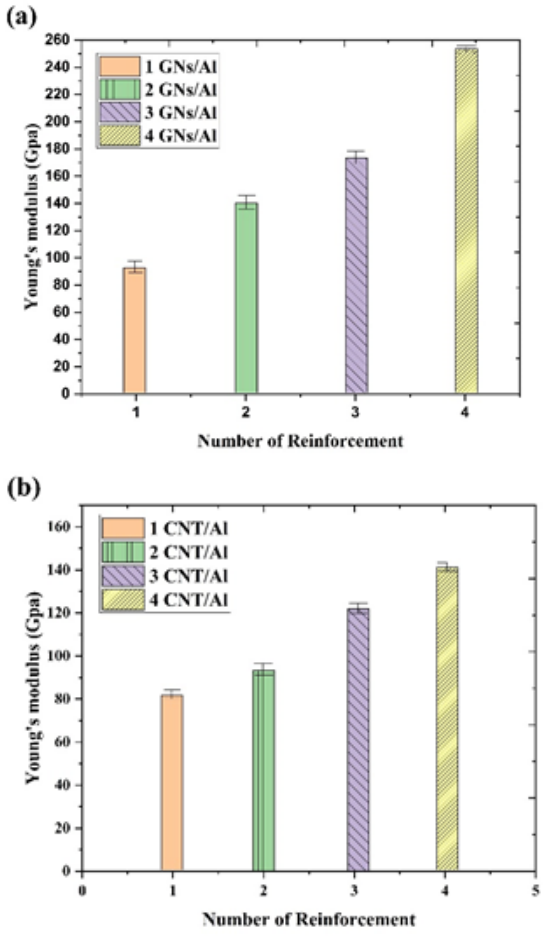

Figure 4. The Young's modulus of the nanocomposite under the number of graphene and carbon nanotube reinforcements (a) GNs/Al nanocomposites (b) CNT/Al nanocomposites.

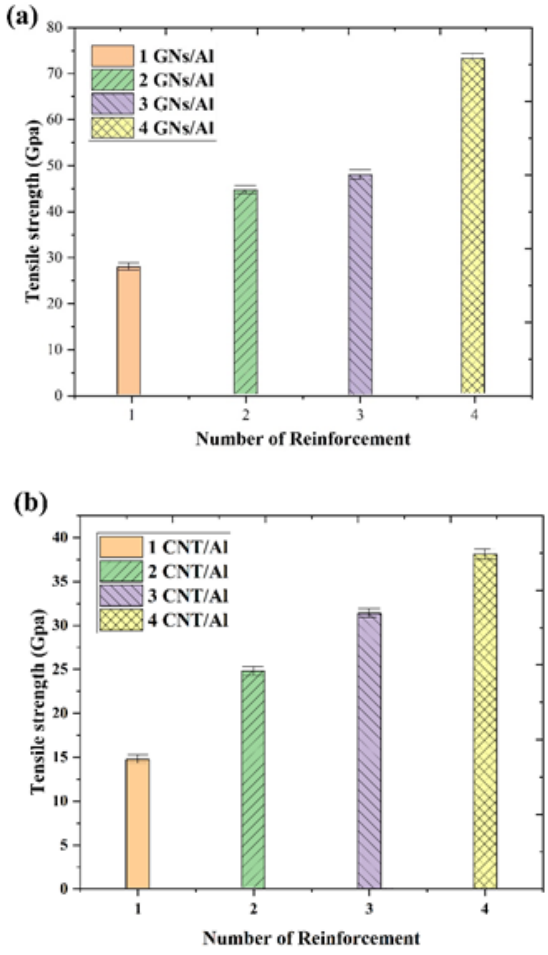

Figure 5. The tensile strength of the nanocomposite under the number of graphene and carbon nanotube reinforcements (a) GNs/Al nanocomposites (b) CNT/Al nanocomposites.

of nanocomposites increased from 14 to 37.5 GPa. By increasing the number of reinforcements (graphene nanoplates and carbon nanotubes), which can increase the electrostatic and Van der Waals forces between the reinforcement and the matrix. As a result, the amount of strength increases in young modules. The results obtained from the effect of increasing the number of graphene nanosheets of nanocomposites on the mechanical properties of tensile strength and Young's modulus are in agreement with the results of [39]. Also, in Table 1, the amount of Young's modulus obtained from aluminum nanocomposites reinforced with a graphene nanoplate as well as a carbon nanotube is in good agreement with the Young's modulus results (MD and experimental methods) of the Rong et al. [43] and Choi et al. [34], respectively. In addition, Temperature jumps often occur in molecular dynamics (MD) simulations, with varying intensities at different locations due to statistical mechanics and thermal runaway effects. Machine Learning Interatomic Potentials (MLIPs) can be utilized to enhance the accuracy of results and minimize these errors. This approach leverages machine learning to develop interatomic potentials, enabling precise prediction of the mechanical properties of nanocomposites [45].

Table 1. Comparing Young's modulus of aluminum nanocomposites.

Nanocomposites	Number of reinforcements	Young's modulus (GPa)	Methods	Ref.
CNT (4,4)/Al	1	75.59 – 94.08	MD	[34]
GNs/Al	1	74.78 – 87.21	MD	[43]
GNs/Al	1	82.48 – 87.93	Experimental	[44]
CNT (4,4)/Al	1	79	MD	This study
GNs/Al	1	88	MD	This study

3.2 Effect of defects in nano-reinforcers on the mechanical properties of aluminum nanocomposites

Figure 6 shows the graphs of strain stress curves of aluminum nanocomposites with defective graphene nanosheets. According to figure 6 (a), the amount of tensile strength increases with the increase of graphene nanosheets. Also, figure 6 (b), for carbon nanotubes, the amount of strength increases with the increase of the number of nanotubes in the aluminum matrix. In addition, figure 7 shows the changes in Young's modulus of aluminum nanocomposites reinforced with a number of carbon nanotubes and graphene sheets (white and without defects). According to figure 7 (a), the lowest amount of Young's modules related to single-layer graphene with defects is 79 GPa. Also, the highest amount of Young's modulus for 4-layer graphene is 52 GPa. By comparing different nanocomposites in figure 7 (a), nanocomposites reinforced with graphene (without defects) nanosheets have higher strength and Young's modulus than nanocomposites reinforced with defective graphene nanosheets. Also, in figure 7 (b) shows nanocom-

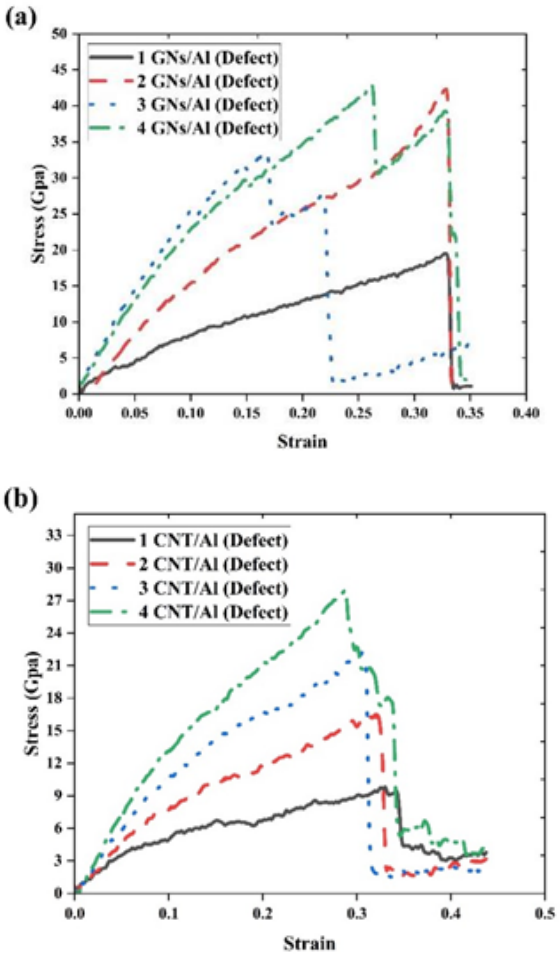

Figure 6. The strain stress curves of aluminum nanocomposites with defective graphene nanosheets and carbon nanotubes (a) GNs/Al nanocomposites (b) CNT/Al nanocomposites.

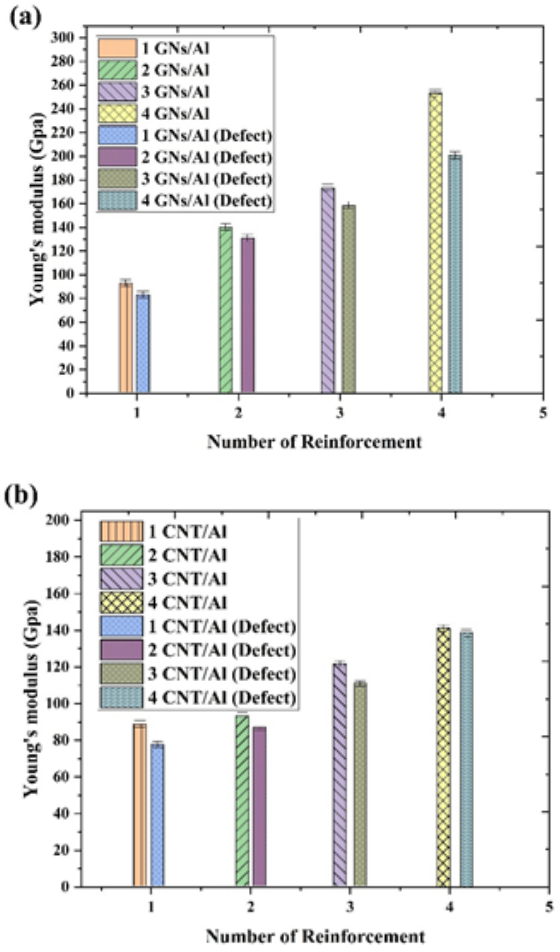

Figure 7. The Young's modulus of aluminum nanocomposites reinforced with a number of carbon nanotubes and graphene sheets (white and without defects) (a) GNs/Al nanocomposites (b) CNT/Al nanocomposites.

posites reinforced with defective carbon nanotubes. According to the graph of figure 7 (b), the lowest Young's modulus of the aluminum nanocomposite reinforced with a defective carbon nanotube is 67 GPa. Also, the highest Young's modulus of the nanocomposite reinforced with 4 carbon nanotubes is equal to 138. By comparing the Young's modulus of aluminum reinforced with carbon nanotubes (with and without defects), their results showed that nanocomposites reinforced with defective carbon nanotubes have a lower Young's modulus than carbon nanotubes without defects.

Figure 8 shows the tensile strength of aluminum nanocomposites reinforced with graphene nanosheets and carbon nanotubes (with and without defects). By increasing the number of graphene and carbon nanotubes (with and without defects), the amount of tensile strength increases (figures 8 (a) and 8 (b)). By comparing the tensile strength of aluminum nanocomposites reinforced with carbon nanotubes and graphene nanoplates (with and without defects), nanocomposites that have one reinforcement of defective carbon tubes and defective graphene nanoplates have a lower tensile strength than nanocomposites reinforced with carbon nanotubes and graphene nanoplates without defects. The presence of defects in the reinforcements (carbon nanotubes and graphene nanosheets) due to the breaking of a number of covalent bonds between carbon atoms causes a decrease in the strength of the nano-reinforcers and ultimately. So, strength and Young's modulus of aluminum nanocomposites decrease. The obtained results of the effect of defects in nano-reinforcers on the mechanical properties (Young's model strength) of nanocomposites were in good agreement with the results of Li et al. [46].

3.3 Effect of temperature on the mechanical properties of aluminum nanocomposites reinforced with graphene nanosheets and carbon nanotubes

Figure 9 shows the stress-strain curves of aluminum nanocomposites reinforced with graphene nanoplates (with and without defects) under different temperatures (250 to 500° K). According to the diagrams of figures 9 (a), (b), (c) and (d), the strength of nanocomposites decreases with increasing temperature. The lowest level of strength for aluminum nanocomposites reinforced with defective graphene nanoplates is at 500° K, and the highest level of strength is related to graphene nanoplates (without defects) at 250° K. Also, in figures 9 (a), (b), (c) and (d) also show the stress-strain graphs for aluminum nanocomposites reinforced with graphene nanosheets (with and without defects) in the form of two layers, three layers, and four layers under different temperatures. The results of these graphs also show that with increasing temperature, the strength of aluminum nanocomposites decreases. Figure 10 shows the stress-strain curves of aluminum nanocomposites reinforced with carbon nanotubes (with defects) under different temperatures. In figures 10 (a), (b), (c) and (d), are the order for nanocomposites reinforced with 1, 2, 3 and 4 carbon nanotubes (with and without defects). According to Figure 10 (a), (b), (c) and (d), with increasing temperature, the strength of nanocomposites decreases. Also, by comparing aluminum nanocomposites reinforced with carbon nanotubes (with and without defects), nanocomposites reinforced with defective carbon nanotubes have a greater reduction in strength than aluminum nanocomposites reinforced with carbon nanotubes without defects.

The increase in temperature in nanocomposites due to the increase in kinetic energy between atoms decreases electrostatic and van der Waals forces between the aluminum matrix and graphene nanosheets as well as carbon nanotubes. Therefore, strength and Young's modulus of the nanocomposite decrease. The results obtained from the effect of increasing temperature on the mechanical properties of Young's model in this study were consistent with the results obtained by [38, 47]. In addition, by increasing the temperature in nanocomposite models, the system becomes more ductile, leading to the development of a BVP on a macro scale during failure. To address this challenge, Talebi et al. [48] proposed a discontinuous semi-concurrent method that employs a cohesive law for cracks.

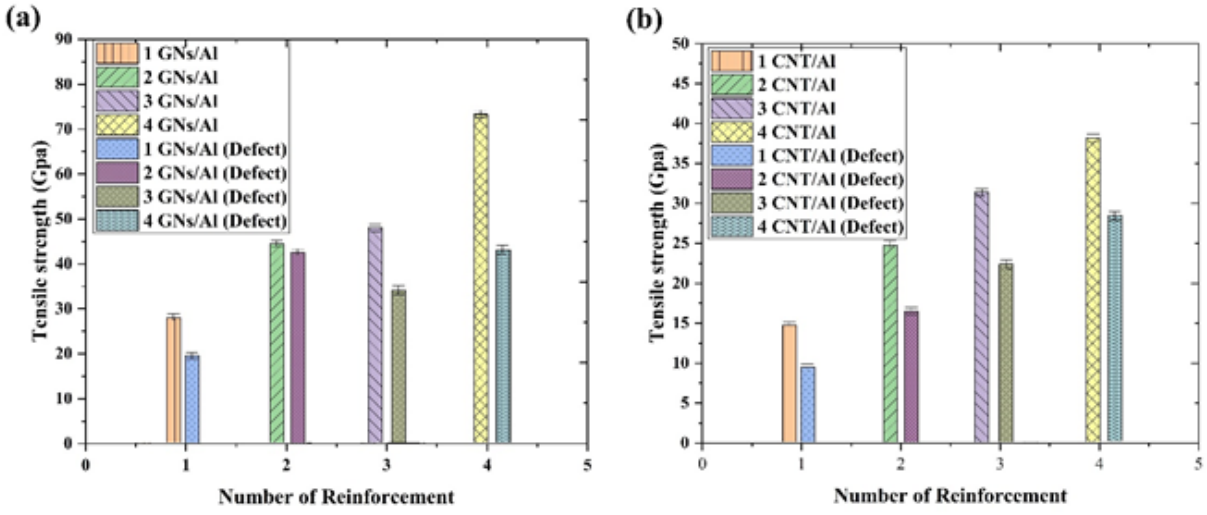

Figure 8. The tensile strength of aluminum nanocomposites reinforced with graphene nanosheets and carbon nanotubes (with and without defects) (a) GNs/Al nanocomposites (b) CNT/Al nanocomposites.

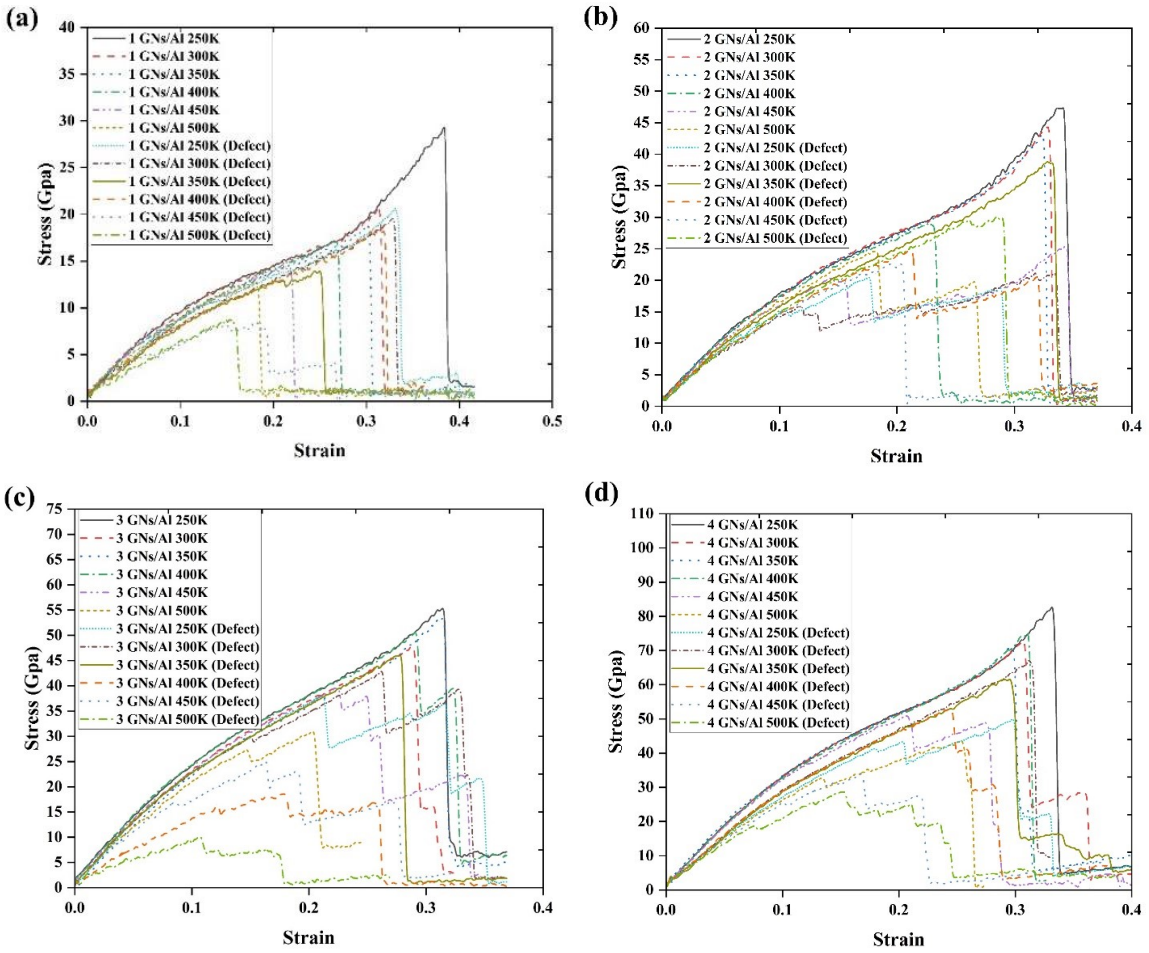

Figure 9. The stress-strain curves of aluminum nanocomposites reinforced with graphene nanoplates (with and without defects) under different temperatures (a) 1 GNs/Al nanocomposites (b) 2 GNs/Al nanocomposites (c) 3 GNs/Al nanocomposites (d) 4 GNs/Al nanocomposites.

3.4 Effect of different strain rates and critical energy release rate

Figure 11 shows the stress-strain curve diagrams of nanocomposites under different strain rates. Figure 11 (a) shows the stress-strain diagrams of aluminum nanocomposites reinforced with graphene nanosheets under different strain rates. Figure 11 (a) shows that with increasing strain rate (0.001 to 0.1 Ps^{-1}), the ultimate tensile strength decreases. In addition, figure 11 (b) shows the stress-strain curves of aluminium nanocomposites reinforced by carbon nanotubes under different strain rates. According to the curves in figure 11 (b), with increasing strain rate, the ultimate tensile strength decreases. According to the curves in figure 11 (b), with increasing strain rate, the ultimate tensile strength decreases. Similarly, figures 11 (c) and 11 (d) show the stress-strain curves of nanocomposites reinforced with graphene nanosheets and carbon nanotubes (with defects), respectively. According to these diagrams, with increasing strain rate, the ultimate tensile strength decreases. In addition, Table 2 shows the Young's modulus of different nanocomposites under different strain rates (0.001 to 0.1 Ps^{-1}). According to Table 2, as the strain rate increases in nanocomposites, Young's modulus of nanocomposites decreases. According to Table 2, the highest Young's modulus of aluminum nanocomposites reinforced with 4 graphene nanosheets and 4 carbon nanotubes were 252 and 138 GPa under the 0.001 Ps^{-1} strain rate, respectively. Also, the lowest Young's modulus of nanocomposites reinforced with 1 graphene nanosheet and 1 carbon nanotube (with defects) were 69 and 67 GPa under the 0.1 Ps^{-1} strain rate, respectively. In addition, Table 2 shows the critical energy release rates of nanocomposites. According to Table 2, by increasing the number of reinforcements in nanocomposites, the critical energy release rate increases. According to Table 2, the highest critical energy release rates of aluminum nanocomposites reinforced with 4 graphene nanosheets and 4 carbon nanotubes were 88.61 and 49.56 J/m^2, respectively. Also, the lowest critical energy release rates of aluminum nanocomposites reinforced with 1 graphene nanosheet and 1 carbon nanotube (with defect) were 69 and 67 J/m^2, respectively.

3.5 Investigating the radial distribution function in aluminum nanocomposites

Figure 12 shows graphs of the radial distribution function between aluminum and carbon atoms in aluminum nanocomposites reinforced with graphene nanosheets and carbon nanotubes. Figures 12 (a) and (c), shows the graph of the radial distribution function for aluminum reinforced with graphene (with and without defects). The results of

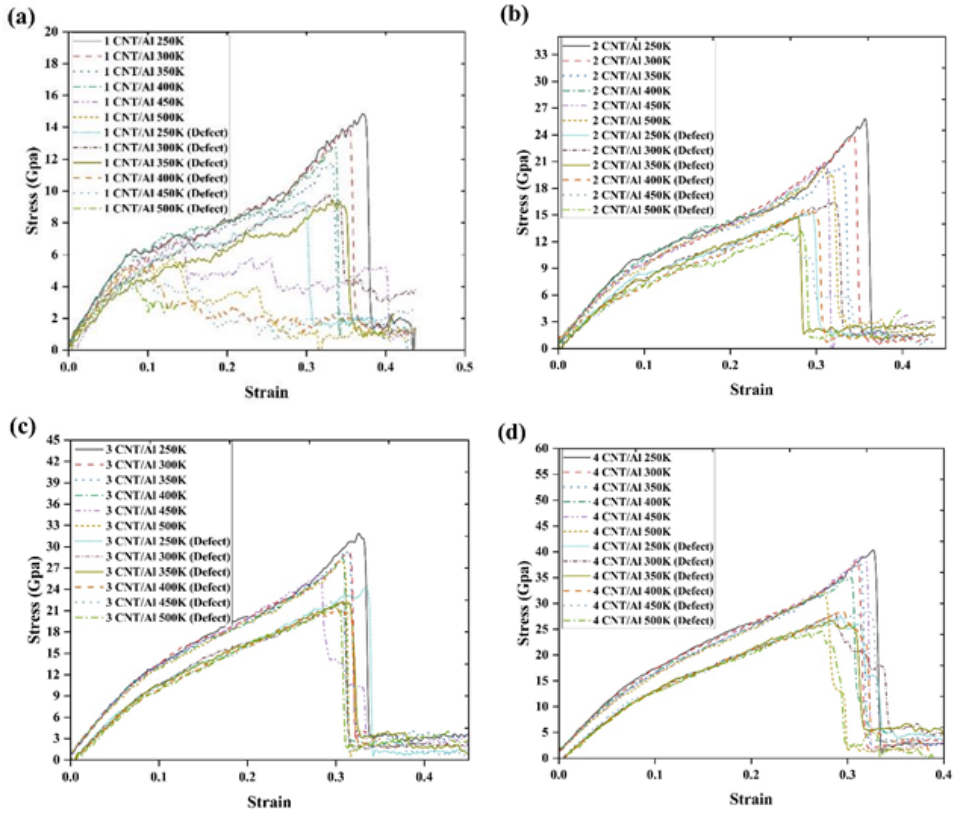

Figure 10. The stress-strain curves of aluminum nanocomposites reinforced with carbon nanotubes (with and without defects) under different temperatures (a) 1 CNT/Al nanocomposites (b) 2 CNT/Al nanocomposites (c) 3 CNT/Al nanocomposites (d) 4 CNT/Al nanocomposites.

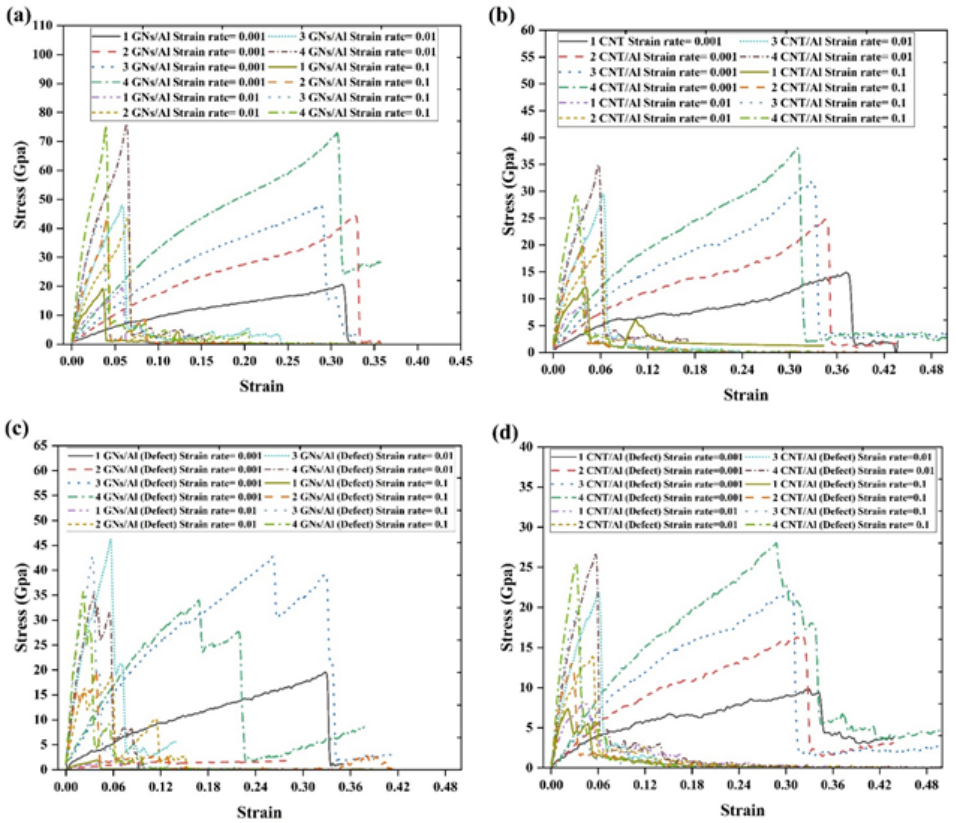

Figure 11. Stress-strain curve of Nanocomposites under the different strain rate 0.001, 0.01, 0.1 Ps^{-1} (a) GNs/Al (b) CNT/Al (c) GNs/Al (with defect) (d) CNT/Al (with defect).

Table 2. Young's modulus and Critical energy release rates of nanocomposites.

Nanocomposites	Number of Reinforcements	Young's modulus (Gpa)			Critical Energy Release Rate (J/m^2)
		$0.001\ Ps^{-1}$	$0.01\ Ps^{-1}$	$0.1\ Ps^{-1}$	
GNs/Al	1	88	83	79	21.36
GNs/Al	2	135	129	124	38.31
GNs/Al	3	174	168	144	64.81
GNs/Al	4	252	246	239	88.61
GNs/Al (Defect)	1	78	72	69	17.20
GNs/Al (Defect)	2	130	124	118	36.31
GNs/Al (Defect)	3	151	144	138	56.8
GNs/Al (Defect)	4	212	206	201	78.40
CNT/Al	1	83	77	74	17.52
CNT/Al	2	93	87	83	33.10
CNT/Al	3	121	115	109	39.21
CNT/Al	4	138	131	125	49.56
CNT/Al (Defect)	1	78	72	67	14.71
CNT/Al (Defect)	2	89	83	78	25.21
CNT/Al (Defect)	3	116	108	102	33.5
CNT/Al (Defect)	4	133	127	122	45.81

these graphs show that by increasing the number of nano-reinforcements by 1 to 4, the interaction between aluminum and carbon atoms increases. Also, comparing figures 12 (a) and 12 (c), nanocomposites reinforced with graphene (without defects) have more proximity (interaction) of aluminum and carbon atoms than aluminum composites reinforced with graphene nanosheets with defects. Also, figures 12 (b) and 12 (d) show aluminum nanocomposites reinforced with the carbon nanotubes (with and without defects). The results of these graphs (figures 12 (b) and 12 (d)) show that

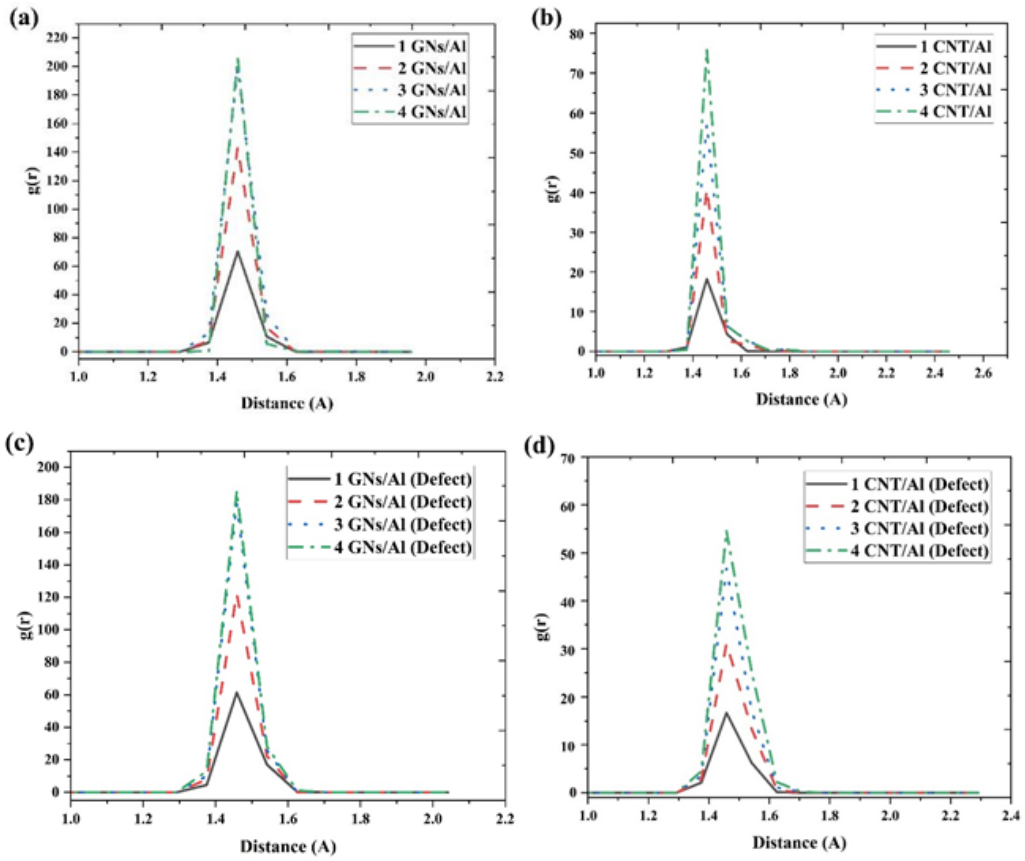

Figure 12. The radial distribution function between aluminum and carbon atoms in aluminum nanocomposites reinforced with graphene nanosheets and carbon nanotubes (a) GNs/Al nanocomposites without defects (b) CNT/Al nanocomposites without defects (c) GNs/Al nanocomposites with defects (d) CNT/Al nanocomposites with defects.

by increasing the number of carbon nanotubes (with and without defects) in aluminum nanocomposites, aluminum atoms interact more closely with carbon. Also, by comparing figures 12 (b) and (d), aluminum nanocomposites reinforced with carbon nanotubes (without defects) have more interaction and proximity between aluminum and carbon atoms than aluminum nanocomposite reinforced with carbon nanotubes with defects. In addition, according to the diagrams in figure 12, all nanocomposites have reached equilibrium because g(r) tends to a constant number as the distance increases.

4. Conclusion

In this study, molecular dynamics simulation was used to investigate the effect of the number of graphene nanoplates and carbon nanotubes (with and without defects) in the aluminum matrix. The results show that the tensile strength and Young's modules improved by increasing the number of graphene nanoplates and carbon nanotubes in the aluminum matrix. The highest Young's modulus was related to aluminum nanocomposite reinforced with 4 graphene nanoplates equal to 252 GPa and 4 carbon nanotubes equal to 138 GPa. Also, the lowest amount was related to the aluminum nanocomposite reinforced with one graphene nanoplate equal to 88 GPa and the aluminum nanocomposite reinforced with one carbon nanotube equaled 79 GPa. In addition, the presence of structural defects in graphene nanosheets and carbon nanotubes reduces the Young's modulus and tensile strength of nanocomposites. In addition, with increasing temperature from 250 to 500° K, the tensile strength and Young's modulus of nanocomposites decrease. Also, the lowest amount of strength and Young's modulus of nanocomposites occurs at 500° K, and also the highest amount of tensile strength was at 250° K.

Authors contributions
Authors have contributed equally in preparing and writing the manuscript.

Availability of data and materials
The authors declare that the data supporting the findings of this study are available within the paper.

Conflict of interests
The authors assert that they do not have any identifiable conflicting financial interests or personal relationships that might be perceived to influence the work presented in this paper.

References

[1] D. Ashkenazi. "How aluminum changed the world: A metallurgical revolution through technological and cultural perspectives.". *Technol Forecast Soc Change*, 143:101–13, 2019.
DOI: https://doi.org/10.1016/j.techfore.2019.03.011.

[2] G. Cole and A. Sherman. "Light weight materials for automotive applications.". *Mater Charact.*, 35:3–9, 1995.
DOI: https://doi.org/10.1016/1044-5803(95)00063-1.

[3] H. M. Lee, S. Y. Choi, A. Jung, and S. H. Ko. "Highly conductive aluminum textile and paper for flexible and wearable electronics.". *Angew Chem.*, 125:7872–7, 2013.
DOI: https://doi.org/10.1002/anie.201301941.

[4] S. Mancin, C. Zilio, L. Rossetto, and A. Cavallini. "Heat transfer performance of aluminum foams.". *J Heat Mass Transf.*, 133:060904, 2011.
DOI: https://doi.org/10.1115/1.4003451.

[5] W. A. de Morais, L. C. R. Lima, H. D. S. Junior, and M. de Morais Tavares. "Improvement of Safety in the use of Aluminum Platforms for Civil Construction.". *Unisanta Science and Technology*, 8:75–84, 2020. URL http://periodicos.unisanta.br/index.php/sat.

[6] D. Dordevic, H. Buchtova, S. Jancikova, B. Macharackova, M. Jarosova, T Vitez, et al. "Aluminum contamination of food during culinary preparation: Case study with aluminum foil and consumers' preferences.". *Food Sci Nutr.*, 7:3349–60, 2019.
DOI: https://doi.org/10.1002/fsn3.1204.

[7] B. Wang, G. Xie, L. Wu, P. Xue, D. Ni, B. Xiao, et al. "Grain size effect on tensile deformation behaviors of pure aluminum.". *Mater Sci amp; Eng A: Struct Mater: Prop Microstruct Process*, 820:141504, 2021.
DOI: https://doi.org/10.1016/j.msea.2021.141504.

[8] M. Sadjadi, M. Meskinfam, B. Sadeghi, H. Jazdarreh, and K. Zare. "In situ biomimetic synthesis and characterization of nano hydroxyapatite in gelatin matrix.". *J Biomed Nanotechnol*, 7:450–4, 2011.
DOI: https://doi.org/10.1166/jbn.2011.1305.

[9] M. S. Sadjadi, B. Sadeghi, and K. Zare. "Natural bond orbital (NBO) population analysis of cyclic thionylphosphazenes,[NSOX $(NPCl_2)_2$]; X= F(1), X= Cl(2).". *J Mol Struct THEOCHEM*, 817:27–33, 2007.
DOI: https://doi.org/10.1016/j.theochem.2007.04.015.

[10] B. Sadeghy and S. Ghammami. "Oxidation of alcohols with tetramethylammonium fluorochromate in aceticoi acid. ". *Russ J Gen Chem.*, 75:1886–8, 2005.
DOI: https://doi.org/10.1007/s11176-006-0008-0.

[11] A. Amininia, K. Pourshamsian, and B. Sadeghi. "Nano-ZnO Impregnated on Starch-A Highly Efficient Heterogeneous Bio-Based Catalyst for One-Pot Synthesis of Pyranopyrimidinone and Xanthene Derivatives as Potential Antibacterial Agents.". *Russ J Org Chem.*, 56:1279–88, 2020.
DOI: https://doi.org/10.1134/S1070428020070234.

[12] B. Sadeghi, S. Ghammamy, Z. Gholipour, M. Ghorchibeigy, and A. A. Nia. "Gold/hydroxypropyl cellulose hybrid nanocomposite constructed with more complete coverage of gold nano-shell.". *Micro & Nano Letters*, 6:209–13, 2011.
DOI: https://doi.org/10.1049/mnl.2011.0036.

[13] A. Salehi and S. Rash-Ahmadi. "Effect of temperature and oxygen functional groups on interaction between epoxy resins and graphene surface.". *Proc Inst Mech Eng C: J Mech Eng Sci.*, 237:941–51, 2023.
DOI: https://doi.org/10.1177/09544062221126626.

[14] A. Kumar, K. Sharma, and A. R. Dixit. "A review on the mechanical properties of polymer composites reinforced by carbon nanotubes and graphene.". *Carbon Lett.*, 31:149–65, 2021.
DOI: https://doi.org/10.1007/s42823-020-00161-x.

[15] A. Kumar, K. Sharma, and A. R. Dixit. "A review on the mechanical and thermal properties of graphene and graphene-based polymer nanocomposites: understanding of modelling and MD simulation.". 46:136–54, 2020.
DOI: https://doi.org/10.1080/0892702220191680844.

[16] A. Yadav, A. Kumar, K. Sharma, and A. Pandey. "Influence of various functional groups in graphene on the mechanical and interfacial properties of epoxy nanocomposites: A review on molecular modeling and MD simulations.". *Int J Comput Mater Sci Eng.*, 11:2250005, 2022.
DOI: https://doi.org/10.1142/S2047684122500051.

[17] A. Kumar, K. Sharma, P. K. Singh, and V. K. Dwivedi. "Mechanical characterization of vacancy defective single-walled carbon nanotube/epoxy composites.". *Mater Today: Proc.*, 4:4013–21, 2017.
DOI: https://doi.org/10.1016/j.matpr.2017.02.303.

[18] A. D. Moghadam, E. Omrani, P. L. Menezes, and P. K. Rohatgi. "Mechanical and tribological properties of self-lubricating metal matrix nanocomposites reinforced by carbon nanotubes (CNTs) and graphene-a review.". *Compos B: Eng.*, 77:402–20, 2015.
DOI: https://doi.org/10.1016/j.compositesb.2015.03.014.

[19] S. Sadeghzadeh, M. Hamzavi, F. Hasheminia, and H. Khashei. "Improving the thermal shock response of aluminum by graphene composition.". *Mater Today Commun.*, 40:110093, 2024.
DOI: https://doi.org/10.1016/j.mtcomm.2024.110093.

[20] S. Sadeghzadeh, M. Hamzavi, and F. Hasheminia. "Improving the mechanical shock response of aluminum by graphene composition: molecular dynamic simulation study.". *Appl Phys A: Mater Sci Process*, 130:1–14, 2024.
DOI: https://doi.org/10.1007/s00339-024-07503-w.

[21] M. Roshan, A. R. Akbarzadeh, S. Sadeghzadeh, and A. Maleki. "ailoring the hardness of aluminum surface reinforced with graphene and C3N nanosheets.". *Diam Relat Mater.*, 127:109139, 2022.
DOI: https://doi.org/10.1016/j.diamond.2022.109139.

[22] K. E. Eshkalak, S. Sadeghzadeh, and F. Molaei. "Aluminum nanocomposites reinforced with monolayer polyaniline (C3N): assessing the mechanical and ballistic properties.". *RSC Adv.*, 10: 19134–48, 2020.
DOI: https://doi.org/10.1039/D0RA03204B.

[23] I. Ahmad, B. Yazdani, and Y. Zhu. "Recent advances on carbon nanotubes and graphene reinforced ceramics nanocomposites.". *Nanomaterials*, 5:90–114, 2015.
DOI: https://doi.org/10.3390/nano5010090.

[24] I. Ovid'Ko. "Mechanical properties of graphene.". *Rev Adv Mater Sci.*, 34:1–11, 2013.

[25] A. Salehi, N. Ghaderiazar, and S. Rash-Ahmadi. "Investigation of thermal conductivity and mechanical properties in multi-layer of graphene and graphene oxide: a molecular dynamics study.". *Mol Simul.*, 50:954–68, 2024.
DOI: https://doi.org/10.1080/08927022.2024.2369710.

[26] P. K. Singh, K. Sharma, A. Kumar, and M. Shukla. "Effects of functionalization on the mechanical properties of multiwalled carbon nanotubes: A molecular dynamics approach.". *J Compos Mater.*, 51: 671–80, 2017.
DOI: https://doi.org/10.1177/0021998316649781.

[27] K. S. Novoselov, A. K. Geim, S. V. Morozov, D-e. Jiang, Y. Zhang, S. V. Dubonos, et al. "Electric field effect in atomically thin carbon films.". *science*, 306:666–9, 2004.
DOI: https://doi.org/10.1126/science.1102896.

[28] A. Salehi and S. Rash-Ahmadi. " Influence of oxygen functional groups on the crack growth behavior of graphene with edge and middle crack: A molecular dynamics study.". *Proc Inst Mech Eng N: J Nanomater Nanoeng Nanosyst.*, 2024.
DOI: https://doi.org/10.1177/23977914231217920.

[29] Y. Jiang, R. Xu, Z. Tan, G. Ji, G. Fan, Z. Li, et al. "Interface-induced strain hardening of graphene nanosheet/aluminum composites.". *Carbon*, 146:17–27, 2019.
DOI: https://doi.org/10.1016/j.carbon.2019.01.094.

[30] M. Morovvati, B. Mollaei-Dariani, S. N. Angili, and D. Toghraie. "The effects of single-walled carbon nanotubes dispersion and agglomeration in aluminum matrix: Fabrication and finite element simulation.". *Measurement*, 218:113144, 2023.
DOI: https://doi.org/10.1016/j.measurement.2023.113144.

[31] M. Li and X-W. Lei. "Molecular dynamics studies on mechanical properties and deformation mechanism of graphene/aluminum composites.". *Comput Mater Sci.*, 211:111487, 2022.
DOI: https://doi.org/10.1016/j.commatsci.2022.111487.

[32] Z. Azizi, K. Rahmani, and F. Taheri-Behrooz. "Fatigue life prediction of aluminum-graphene nanocomposites: Application to high-capacity conductors.". *Int J Fatigue*, 175:107749, 2023.
DOI: https://doi.org/10.1016/j.ijfatigue.2023.107749.

[33] S. Zhang, G. Chen, J. Wei, Y. Liu, R. Xie, Q. Liu, et al. "Effects of energy input during friction stir processing on microstructures and mechanical properties of aluminum/carbon nanotubes nanocomposites.". *J Alloys Compd.*, 798:523–30, 2019.
DOI: https://doi.org/10.1016/j.jallcom.2019.05.269.

[34] B. K. Choi, G. H. Yoon, and S. Lee. "Molecular dynamics studies of CNT-reinforced aluminum composites under uniaxial tensile loading.". *Compos B: Eng.*, 91:119–25, 2016.
DOI: https://doi.org/10.1016/j.compositesb.2015.12.031.

[35] V. Khanna, V. Kumar, and S. A. Bansal. "Effect of reinforcing graphene nanoplatelets (GNP) on the strength of aluminium (Al) metal matrix nanocomposites.". *Mater Today: Proc.*, 61:280–5, 2022.
DOI: https://doi.org/10.1016/j.matpr.2021.09.227.

[36] M. Motamedi, A. Naghdi, and S. Jalali. "Effect of temperature on properties of aluminum/single-walled carbon nanotube nanocomposite by molecular dynamics simulation.". *Proc Inst Mech Eng C: J Mech Eng Sci.*, 234:635–42, 2020.
DOI: https://doi.org/10.1177/0954406219878760.

[37] S. Dixit, A. Mahata, D. R. Mahapatra, S. V. Kailas, and K. Chattopadhyay. "Multi-layer graphene reinforced aluminum-manufacturing of high strength composite by friction stir alloying.". *Compos B: Eng.*, 136:63–71, 2018.
DOI: https://doi.org/10.1016/j.compositesb.2017.10.028.

[38] J. Huang, M. Li, J. Chen, Y. Cheng, Z. Lai, J. Hu, et al. "Effect of Temperatures and Graphene on the Mechanical Properties of the Aluminum Matrix: A Molecular Dynamics Study.". *Materials*, 16: 2722, 2023.
DOI: https://doi.org/10.3390/ma16072722.

[39] X. Wang, W. Xiao, L. Wang, J. Shi, L. Sun, J. Cui, et al. "Investigation on mechanical behavior of multilayer graphene reinforced aluminum composites.". *Phys E: Low-Dimens Syst Nanostructures*, 123:114172, 2020.
DOI: https://doi.org/10.1016/j.physe.2020.114172.

[40] J. Tersoff. "New empirical approach for the structure and energy of covalent systems.". *Phys Rev B.*, 37:6991, 1988.
DOI: https://doi.org/10.1103/PhysRevB.37.6991.

[41] M. S. Daw and M. I. Baskes. "Embedded-atom method: Derivation and application to impurities, surfaces, and other defects in metals. ". *Phys Rev B.*, 29:6443, 1984.
DOI: https://doi.org/10.1103/PhysRevB.29.6443.

[42] S. Plimpton. "Fast parallel algorithms for short-range molecular dynamics.". *J Comput Phys.*, 117:1–19, 1995.
DOI: https://doi.org/10.1006/jcph.1995.1039.

[43] Y. Rong, H. He, L. Zhang, N. Li, and Y. Zhu. "Molecular dynamics studies on the strengthening mechanism of Al matrix composites reinforced by grapnene nanoplatelets.". *Comput Mater Sci.*, 153: 48–56, 2018.
DOI: https://doi.org/10.1016/j.commatsci.2018.06.023.

[44] L. Yolshina, R. Muradymov, D. Vichuzhanin, and E. Smirnova. "Enhancement of the mechanical properties of aluminum-graphene composites.". *AIP Conf Proc: AIP Publishing.*, 2016.
DOI: https://doi.org/10.1063/1.4967150.

[45] B. Mortazavi, M. Silani, E. V. Podryabinkin, T. Rabczuk, X. Zhuang, and A. V. Shapeev. "First-principles multiscale modeling of mechanical properties in graphene/borophene heterostructures empowered by machine-learning interatomic potentials.". *Adv Mater.*, 33:2102807, 2021.
DOI: https://doi.org/10.1002/adma.202102807.

[46] D. Li, S. Song, D. Zuo, and W. Wu. "Effect of pore defects on mechanical properties of graphene reinforced aluminum nanocomposites.". *Metals*, 10:468, 2020.
DOI: https://doi.org/10.3390/met10040468.

[47] A. Salehi and S. Rash-Ahmadi. "Effect of adsorption, hardener, and temperature on mechanical properties of epoxy nanocomposites with functionalized graphene: A molecular dynamics study.". *J Mol Graph Model*, 117:108311, 2022.
DOI: https://doi.org/10.1016/j.jmgm.2022.108311.

[48] H. Talebi, M. Silani, S. P. Bordas, P. Kerfriden, and T. Rabczuk. "A computational library for multiscale modeling of material failure.". *Comput Mech*, 53:1047–71, 2014.
DOI: https://doi.org/10.1007/s00466-013-0948-2.